Synthesis and magnetic properties of FePt-B nanocomposite permanent magnets with low Pt concentrations

doi: 10.1063/1.1824172

Synthesis and magnetic properties of Fe–Pt–B nanocomposite permanent magnets with low Pt concentrations

Wei Zhang,[a] Dmitri V. Louzguine, and Akihisa Inoue
Institute for Materials Research, Tohoku University, Sendai 980-8577, Japan

(Received 10 May 2004; accepted 22 September 2004)

Microstructure and magnetic properties of melt-spun $Fe_{80-x}Pt_xB_{20}$ ($x=20,22,24$) alloy ribbons have been investigated. A homogeneous nanoscale mixed structure with amorphous and fcc γ-FePt phases was formed in the melt-spun ribbons. The average sizes of the amorphous and fcc γ-FePt phases are about 5 nm, and the enrichment phenomenon of B is recognized in the coexistent amorphous phase. The melt-spun ribbons exhibit soft magnetic properties. The nanocomposite structure consisting of fct γ_1-FePt, fcc γ-FePt, and Fe_2B phases was obtained in the melt-spun ribbons annealed at 798 K for 900 s, and their average grain sizes are about 20 nm. The remanence (B_r), reduced remanence (M_r/M_s), coercivity ($_iH_c$), and maximum energy product $(BH)_{max}$ of the nanocomposite alloys are in the range of 0.93–1.05 T, 0.79–0.82, 375–487 kA/m, and 118–127 kJ/m^3, respectively. The good hard magnetic properties are interpreted as resulting from exchange magnetic coupling between nanoscale hard fct γ_1-FePt and soft magnetic fcc γ-FePt or Fe_2B phases. © *2004 American Institute of Physics*. [DOI: 10.1063/1.1824172]

Fe–Pt alloys have gained much interest for the appearance of permanent magnetic characteristics[1–5] resulting from an $L1_0$ order faced-centered tetragonal FePt phase (fct γ_1-FePt) with very high magnetic crystalline anisotropy ($K=7$ MJ m^{-3}).[6] The Fe–Pt alloys prepared by casting exhibit a maximum energy product $(BH)_{max}$ of 160 kJ/m^3 [2] and the $(BH)_{max}$ further increases to 240 kJ/m^3 in sputtered Fe–Pt thin films.[4,5] Recently, Fe–Pt nanocomposites have drawn much attention. Thang *et al.*[7] made Fe–Pt nanocomposite magnets by casting and annealed them at 1598 K. They obtained a maximum energy product of 132 kJ/m^3. Liu *et al.*[8] reported that the Fe–Pt nanocomposite films prepared by sputtering and then rapid annealing exhibited a maximum energy product close to 320 kJ/m^3. In nanocomposite magnets, the sizes of both hard and soft magnetic phases are in the nanoscale range so that the magnetic moments of adjacent grains are exchange-coupled, leading to an enhanced energy product.[9] Various techniques such as melt spinning,[10–12] sputtering,[8,13] mechanical alloying,[14,15] and casting[7,16] now have provided an ample scope for fabrication of nanocomposite thin films and bulks. Among the above-mentioned techniques, the melt-spinning is very useful for preparation of nanocomposite materials because the amorphous (or nanocrystalline) structure of the ribbons can be easily crystallized to nano-sized grains by subsequent heat treatment. However, there has been no report on the realization of Fe–Pt nanocomposite alloys having good hard magnetic properties by melt quenching. The absence of eutectic point over the entire composition range in Fe–Pt binary alloy system hinders the formation of high quality ribbons from the melt.[17] This problem can be solved by the application of the three component rule,[18,19] which is well known for fabrication of bulk amorphous alloys. According to this rule, the addition of third element to the Fe–Pt binary alloy is expected to result in the production of high quality amorphous ribbons.

The Fe–Pt binary alloys with good hard magnetic properties contain 38–50 at.% Pt because the larger amount of fct γ_1-FePt phase is formed in the composition range above 35 at.% Pt through order-disorder transformation.[2,20] The high Pt contents lead to high materials cost. For extension of application fields, it is important to reduce Pt content without detriment to good hard magnetic properties. Inomata *et al.*[21] has reported that the addition of boron to Fe–Pt alloys expands the fct γ_1-FePt phase field to lower composition range. However, no nanocomposite alloys with good hard magnetic properties have been obtained in the Fe–Pt–B system. In this letter we report the microstructure and magnetic properties of Fe–Pt–B melt-spun ribbons with lower Pt contents in as-spun and annealed states, and the formation of nanocomposite structure containing the fct γ_1-FePt phase with excellent hard magnetic properties.

Alloy ingots with composition of $Fe_{80-x}Pt_xB_{20}$ ($x=20,22,24$) were prepared by arc melting the mixtures of pure Fe (99.9 mass%), Pt (99.95 mass%) and boron (99.5 mass%) in an argon atmosphere. The ingot was crushed into small pieces to accommodate the size of a quartz crucible for melt spinning. The nozzle diameter of the crucible was about 0.5 mm. Ribbons were produced by melt spinning at a wheel circumferential speed of 45 m/s in an argon atmosphere. These ribbons were sealed in a quartz tube, evacuated to 2×10^{-3} Pa and then isothermally annealed for 900 s at 723–873 K. The structure of the ribbons was examined by x-ray diffraction (Cu $K\alpha$) and transmission electron microscopy (TEM) linked energy dispersive spectroscopy (EDS) using an electron beam of ~5 nm. The EDS was used for analyzing the composition of the phases. Thermal stability was investigated under an Ar atmosphere at a heating rate of 0.67 K/s by differential scanning calorimetry (DSC). Magnetic properties were measured by a vibrating sample magnetometer with a maximum applied magnetic field of 1274 and 3980 kA/m. The coercive force of the $Fe_{80-x}Pt_xB_{20}$ ribbons in as-spun state was measured with a $B-H$ loop tracer. The density of the $Fe_{80-x}Pt_xB_{20}$ ribbons was determined as 11.059–11.643 Mg/m^3 by the Archimedean method using toluene.

[a]Author to whom correspondence should be addressed; electronic mail: wzhang@imr.tohoku.ac.jp

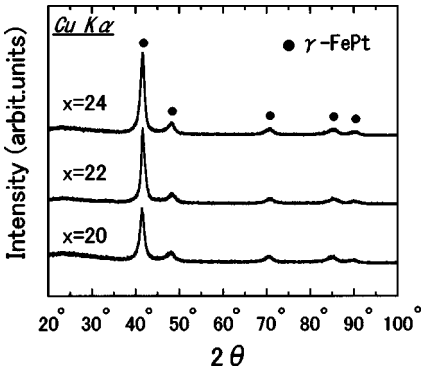

FIG. 1. X-ray diffraction patterns of melt-spun $Fe_{80-x}Pt_xB_{20}$ ($x=20,22$, and 24) ribbons.

Figure 1 shows x-ray diffraction patterns of the melt-spun $Fe_{80-x}Pt_xB_{20}$ ($x=20,22,24$) alloy ribbons. The diffraction pattern can be identified as a fcc γ-FePt phase, but their diffraction peaks are relatively broad, indicating that the ribbons consist of nanometer-sized crystalline phases. The high-resolution transmission electron microscopy image of the as-spun $Fe_{58}Pt_{22}B_{20}$ ribbon is shown in Fig. 2. One can observe a homogeneous nanoscale mixed structure consisting of amorphous and fcc γ-FePt phases. The average sizes of the amorphous and fcc γ-FePt phases are measured as about 5 nm, and the volume fraction of the amorphous phase is estimated to be approximately 40%. The EDS analysis reveals an average composition $Fe_{51}Pt_{15}B_{34}$ for the amorphous phase and the $Fe_{64}Pt_{33}B_3$ for the fcc γ-FePt phase. It is noticed that the amorphous phase has significantly enriched B concentrations, indicating that the high B contents enhance the amorphous formation ability of the Fe–Pt–B alloy. The DSC curves of the melt-spun $Fe_{80-x}Pt_xB_{20}$ ($x=20,22,24$) ribbons show a distinct exothermic peak. This result also shows that the amorphous phase is included in the ribbon samples, being consistent with the result obtained by TEM. In addition, the heat of crystallization (ΔH_x) of the melt-spun ribbons gradually decreases from 91.0 to 63.5 J/g with increasing Pt content from 20 to 24 at.%, indicating the decrease of the volume fraction of the coexistent amorphous phase in the ribbons.

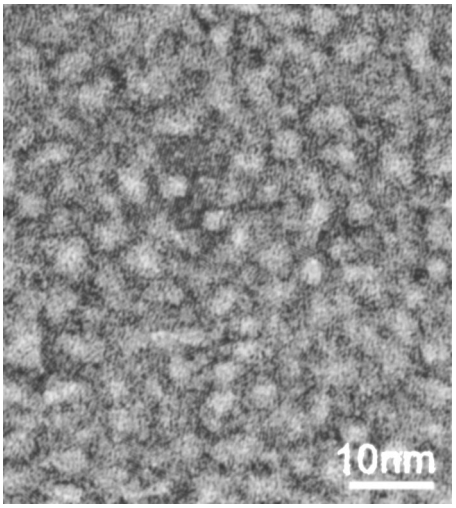

FIG. 2. High-resolution transmission electron microscopy image of a melt-spun $Fe_{58}Pt_{22}B_{20}$ ribbon.

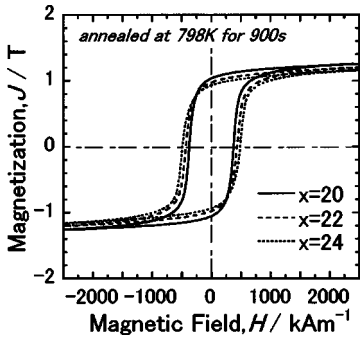

FIG. 3. Hysteresis loops of melt-spun $Fe_{80-x}Pt_xB_{20}$ ($x=20,22$, and 24) ribbons annealed at 798 K for 900 s.

Not any data on the formation of an amorphous phase have been reported for melt-spun Fe–Pt binary alloys. Consequently, it is concluded that the Fe–Pt–B ternary alloys have a higher amorphous-formation ability which exceeds those of the Fe–Pt binary alloys. This can be understood in the framework of the three component rules[18,19] for the achievement of high amorphous-formation ability. The three empirical rules are (1) multicomponent consisting of more than three elements, (2) significant atomic size mismatches above 12%, and (3) suitable negative heats of mixing. In the Fe–Pt–B system, their atomic sizes change in the order of Pt>Fe>B and the atomic size ratios are 1.10 for Pt/Fe, 1.30 for Fe/B, and 1.42 for Pt/B.[22] In addition, the heat of mixing has been estimated to be −13 kJ/mol for Fe–Pt pair, −11 kJ/mol for Fe–B pair, −13 kJ/mol for Pt–B pair.[23] The above-described three component rules are almost completely satisfied for Fe–Pt–B alloys. It is thus interpreted that the increase in amorphous-formation ability by the addition of B to Fe–Pt alloys leads to the homogeneous mixture of amorphous and fcc γ-FePt phases in the melt-spun $Fe_{80-x}Pt_xB_{20}$ ($x=20,22,24$) ribbons.

The $Fe_{80-x}Pt_xB_{20}$ ($x=20,22,24$) alloy ribbons exhibit soft magnetic properties, i.e., saturation magnetization of 1.28–1.32 T and low coercive force of 21.1–49.6 A/m. Figure 3 shows hysteresis loops of the ribbons annealed at 798 K for 900 s. The loops exhibit the achievement of good hard magnetic properties. The remanence (B_r), reduced remanence (M_r/M_s), coercivity ($_iH_c$), and maximum energy product $(BH)_{max}$ of the $Fe_{80-x}Pt_xB_{20}$ ($x=20,22,24$) alloy ribbons annealed at 798 K for 900 s are summarized in Table I. It is seen that the B_r, M_r/M_s, $_iH_c$, and $(BH)_{max}$ are in the range of 0.93–1.05 T, 0.79–0.82, 375–487 kA/m, and 118–127 kJ/m^3, respectively. These materials are magnetically isotropic.

The x-ray diffraction patterns of the melt-spun $Fe_{80-x}Pt_xB_{20}$ ($x=20,22,24$) ribbons annealed at 798 K for 900 s are shown in Fig. 4. The diffraction patterns are identified as fct γ_1-FePt, fcc γ-FePt, and Fe_2B phases for the

TABLE I. Magnetic properties of melt-spun Fe–Pt–B alloys annealed for 798 K for 900 s.

Composition (at.%)	B_r (T)	M_r/M_s	$_iH_c$ (kA/m)	$(BH)_{max}$ (kJ/m^3)
$Fe_{60}Pt_{20}B_{20}$	1.05	0.82	375	127
$Fe_{58}Pt_{22}B_{20}$	0.97	0.81	435	124
$Fe_{56}Pt_{24}B_{20}$	0.93	0.79	487	118

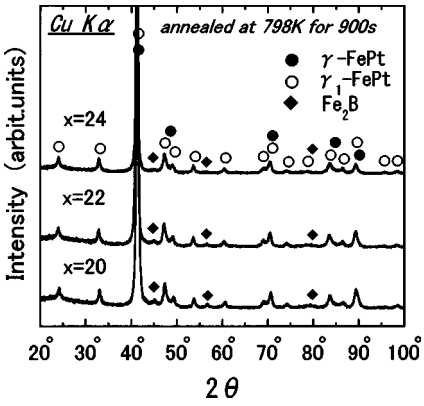

FIG. 4. X-ray diffraction patterns of the melt-spun $Fe_{80-x}Pt_xB_{20}$ ($x=20,22$, and 24) ribbons annealed at 798 K for 900 s.

three samples. Figure 5 shows TEM image and selected-area electron diffraction pattern of the melt-spun $Fe_{58}Pt_{22}B_{20}$ ribbon annealed at 798 K for 900 s. It is recognized that a fine nanocomposite structure is formed and their average grain sizes are about 20 nm. The selected-area electron diffraction pattern indicates that the microstructure is crystallographically isotropic. It is interpreted from the x-ray and TEM data that the fine nanocomposite structure consisting of fct γ_1-FePt, fcc γ-FePt, and Fe_2B phases is formed by annealing of the nanoscale mixed amorphous and fcc γ-FePt phases.

Although the alloys consist of three magnetic components, the hysteresis loop with high remanence value is smooth, being typical of a single component system. The high reduced remanence ($M_r/M_s>0.79$) and reversible demagnetization curves for the isotropic alloy indicate the behavior of the exchange-coupled type magnets.[9] The rather good hard magnetic properties are interpreted to result from exchange magnetic coupling between nanoscale hard fct γ_1-FePt and soft magnetic fcc γ-(FePt) or Fe_2B[24] phases. This may be regarded as a type of Fe–Pt nanocomposite magnet with low contents. In addition, the decrease of B_r and the increase of ${}_iH_c$ with increasing Pt content are presumed to result from the increase in the volume fraction of hard fct γ_1-FePt magnetic phase and the decrease in the volume fraction of soft fcc γ-FePt magnetic phase.

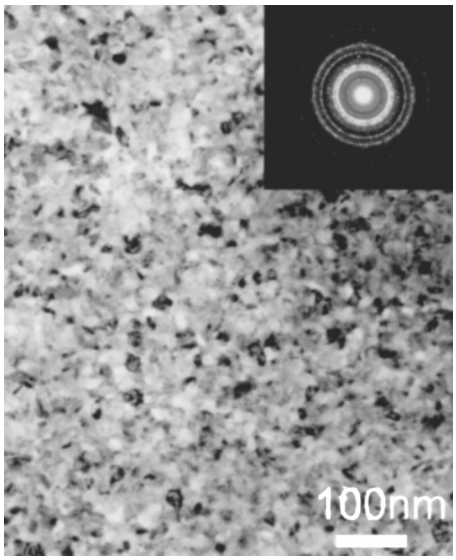

FIG. 5. Transmission electron microscopy image and selected-area electron diffraction pattern of a melt-spun $Fe_{58}Pt_{22}B_{20}$ ribbon annealed at 798 K for 900 s.

In conclusion, the homogeneous nanoscale mixed structure with amorphous and fcc γ-FePt phases was formed in the melt-spun $Fe_{80-x}Pt_xB_{20}$ ($x=20,22,24$) alloy ribbons. The average sizes of the amorphous and fcc γ-FePt phases were about 5 nm. The volume fraction of the amorphous phase gradually decreases with increasing Pt content. The melt-spun ribbons exhibit soft magnetic properties with saturation magnetization of 1.28–1.32 T and lower coercive force of 21.1–49.6 A/m. The nanocomposite structure with fct γ_1-FePt and fcc γ-FePt phases was obtained in the melt-spun ribbons annealed at 798 K for 900 s and the average grain sizes were about 20 nm. The B_r, M_r/M_s, ${}_iH_c$, and $(BH)_{\max}$ of the annealed ribbons are 0.93–1.05 T, 0.79–0.82, 375–487 kA/m, and 118–127 kJ/m^3, respectively. The good hard magnetic properties are interpreted to result from exchange magnetic coupling between nanoscale hard fct γ_1-FePt and soft magnetic fcc γ-FePt or Fe_2B phases. The synthesis of the fct γ_1-FePt/(fcc γ-FePt and Fe_2B) nanocomposite magnets using the melt-spun Fe–Pt–B alloy ribbons with low concentrations is promising for future development of Fe–Pt base hard magnetic materials.

The authors would like to thank Dr. Takako Tsurui at Nanotechnology Support Project of the Ministry of Education, Culture, Science and Technology, Japan for cooperation in analyzing the compositions using the energy dispersive spectroscopy.

[1] A. D. Franklin, A. E. Berkowitz, and E. Klokholm, Phys. Rev. **94**, 1423 (1954).
[2] K. Watanabe and H. Masumoto, Trans. Jpn. Inst. Met. **24**, 627 (1983).
[3] S. W. Yung, Y. H. Chang, T. J. Lin, and M. P. Hung, J. Magn. Magn. Mater. **116**, 411 (1992).
[4] M. Watanabe and M. Homma, Jpn. J. Appl. Phys., Part 2 **35**, L1264 (1996).
[5] J. P. Liu, Y. Liu, C. P. Lou, Z. S. Shan, and D. J. Sellmyer, J. Appl. Phys. **81**, 5644 (1997).
[6] O. A. Ivanov, L. V. Solina, V. A. Demshina, and L. M. Magat, Phys. Met. Metallogr. **35**, 81 (1973).
[7] P. D. Thang, E. Bruck, F. D. Tichelaar, K. H. J. Buschow, and F. R. de Boer, IEEE Trans. Magn. **38**, 2934 (2002).
[8] J. P. Liu, C. P. Lou, Y. Liu, and D. J. Sellmyer, Appl. Phys. Lett. **72**, 483 (1998).
[9] E. F. Kneller and R. Hawig, IEEE Trans. Magn. **27**, 3588 (1991).
[10] R. Coehoorn, D. B. de Mooij, J. P. W. B. Duchateau, and K. H. J. Buschow, J. Phys. C **8**, 669 (1988).
[11] A. Manaf, R. A. Buckley, and H. A. Davis, J. Magn. Magn. Mater. **128**, 302 (1993).
[12] W. Zhang, M. Matsushita, and A. Inoue, J. Appl. Phys. **89**, 492 (2001).
[13] E. E. Fullerton, J. S. Jiang, C. H. Sowers, J. E. Pearson, and S. D. Bader, Appl. Phys. Lett. **72**, 380 (1997).
[14] J. Ding, P. G. McComick, and R. Street, J. Magn. Magn. Mater. **124**, 1 (1993).
[15] K. D. Aylesworth, Z. R. Zhao, D. J. Sellmyer, and G. C. Hadjipanayis, J. Appl. Phys. **64**, 5742 (1988).
[16] W. Zhang and A. Inoue, Appl. Phys. Lett. **80**, 1610 (2002).
[17] B. Giessen. Proceedings of the Fourth International Conference on Rapidly Quenched Metals, Sendai, 1981, p. 213.
[18] A. Inoue: Mater. Trans., JIM **36**, 866 (1995).
[19] A. Inoue: Acta Mater. **48**, 279 (2000).
[20] C. M. Kuo, P. C. Kuo, and H. C. Wu, J. Appl. Phys. **85**, 2264 (1999).
[21] K. Inomata, T. Sawa, andS. Hashimoto, J. Appl. Phys. **64**, 2537 (1988).
[22] *Metals Databook*, edited by Japan Institute Metals of Maruzen, Tokyo, 1983, p. 8.
[23] F. R. Niessen, *Cohesion in Metals* (Elsevier Science, Amsterdam, 1988), pp. 224–225.
[24] O. Crisan, J. M. Le Breton, M. Nogues, F. Machizaud, and G. Filoti, J. Phys.: Condens. Matter **14**, 12599 (2002).